Accepted Manuscript

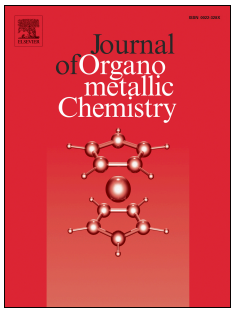

Vanadium olefin polymerization catalysts: NMR spectroscopic characterization of V(III) intermediates

Igor E. Soshnikov, Nina V. Semikolenova, Konstantin P. Bryliakov, Vladimir A. Zakharov, Evgenii P. Talsi

PII: S0022-328X(17)30509-0

DOI: 10.1016/j.jorganchem.2017.08.020

Reference: JOM 20073

To appear in: *Journal of Organometallic Chemistry*

Received Date: 11 August 2017

Revised Date: 29 August 2017

Accepted Date: 31 August 2017

Please cite this article as: I.E. Soshnikov, N.V. Semikolenova, K.P. Bryliakov, V.A. Zakharov, E.P. Talsi, Vanadium olefin polymerization catalysts: NMR spectroscopic characterization of V(III) intermediates, *Journal of Organometallic Chemistry* (2017), doi: 10.1016/j.jorganchem.2017.08.020.

Vanadium olefin polymerization catalysts: NMR spectroscopic characterization of V(III) intermediates

Igor E. Soshnikov [a, b], Nina V. Semikolenova [a], Konstantin P. Bryliakov [a, b], Vladimir A. Zakharov [a, b], Evgenii P. Talsi [a, b, *]

[a] *Federal Agency for Scientific Organizations, Siberian Branch of the Russian Academy of Sciences, Boreskov Institute of Catalysis, 630090, Novosibirsk, Pr. Lavrentieva, 5, Russian Federation*

[b] *The Ministry of Education and Science of the Russian Federation, Novosibirsk State University 630090, Novosibirsk, Pirogova street, 2, Russian Federation*

Abstract

Vanadium(III) species formed upon reacting α-diimine (**1**) and bis(imino)pyridine (**5**) vananadium(III) pre-catalysts with MAO, $AlMe_2Cl$, $AlMe_2Cl/[Ph_3C][B(C_6F_5)_4]$, and $AlMe_3/[Ph_3C][B(C_6F_5)_4]$ have been characterized in detail by ^1H, ^2H, and ^{19}F NMR spectroscopy; the V^{III}-CH_3 moiety has been observed by ^1H and ^2H NMR spectroscopy. For complex **1**, zwitterion-like species $[L'V^{III}R_2^+\cdots MeMAO^-]$ and ion pairs $[L'V^{III}R_2(THF)_2]^+[A]^-$ (L′ = 1,4-bis-3,5-dimethylphenyl-2,3-dimethyl-1,4-diazabuta-1,3-diene; $[A]^-$ = $[MeMAO]^-$ or $[B(C_6F_5)_4]^-$) have been identified. The outer-sphere ion pairs of the type $[L(Cl)V^{III}(\mu\text{-}Cl)_2AlMe_2]^+[A]^-$, $[L(Me)V^{III}(\mu\text{-}Cl)_2AlMe_2]^+[A]^-$, $[LV^{III}Cl_2(THF)]^+[A]^-$ and $[LV^{III}(Cl)Me(THF)]^+[A]^-$ (L = 2,6-bis[1-(2,6-dimethylphenylimino)ethyl]pyridine; $[A]^-$ = $[AlMe_3Cl]^-$ or $[B(C_6F_5)_4]^-$) have been found in the systems based on the complex **5**. The nature of the vanadium species active in ethylene polymerization and the catalyst deactivation pathways are discussed.

Keywords

vanadium, ethylene polymerization, NMR, active species, bis(imino)pyridine, α-diimine

Highlights

• Transient vanadium(III) species have been identified in V^{III} based ethylene polymerization catalyst systems

• The V^{III}-CH_3 moiety has been observed by NMR spectroscopy

• The nature of catalytically active sites and the catalysts deactivation pathways are discussed

1. Introduction

Vanadium-based olefin polymerization catalysts have been used since the 1960th for the production of ethylene/propylene or ethylene/propylene/diene co-polymers (EPM and EPDM rubber). In most cases, the activity and thermal stability of the vanadium-based catalysts is lower than that of zirconium and titanium catalysts, but the former produce polymeric materials with unique properties (amorphous, uniform copolymers), which makes them irreplaceable for the synthetic rubber manufacture [1-5].

"Traditional" pre-catalysts for EPM and EPDM rubber production are VCl_4, $VOCl_3$ and $V(acac)_3$ complexes. In the last 10-15 years, post-metallocene vanadium complexes with various N-, O-and N,O-donor ligands have been extensively studied as pre-catalysts of ethylene homo- and co-polymerization [4-11].

Previously, NMR and EPR techniques were successfully applied for the detection and characterization of the active polymerizing species of the catalyst systems based on Ti, Zr, Hf, Fe, Co, and Ni complexes [12-16]. In contrast, the variety of accessible vanadium oxidation states (0, +1, +2, +3, +4, and +5, most of them being paramagnetic), and low stability of the vanadium-alkyl complexes prevented the identification of the active species in vanadium based catalyst systems [2, 4, 17]. Until recently, the nature of the active species of vanadium-based catalyst systems for olefin polymerization has in fact remained a "black box" [3-5].

Depending on the oxidation state of the vanadium center in the pre-catalyst, trivalent, tetravalent and pentavalent alkyl vanadium complexes have been considered as potential active species of polymerization, while low-valent vanadium species (+2, +1, 0) have been declared as

inactive ones [2, 4, 18-21]. Stable well-characterized vanadium-alkyl complexes have been rather rare in the literature [22-26]; several examples of them are given in Scheme 1. The majority of them are inactive toward olefin polymerization in the absence of aluminum activators.

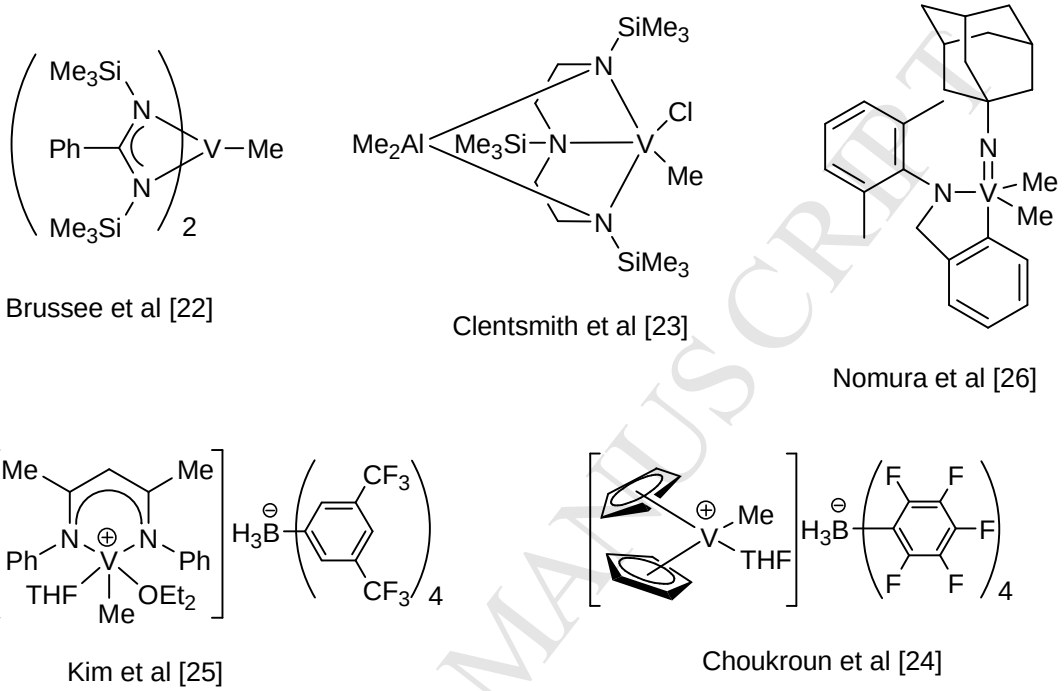

Scheme 1. Structures of well-defined V(III)-alkyl complexes.

Recently, using NMR spectroscopy, we have shown that the activation of different vanadium(III) complexes with bidentate *α*-diimine and tridentate bis(imino)pyridine ligands (Scheme 2) with MAO, $AlMe_3/[CPh_3]^+[B(C_6F_5)_4]^-$, and $AlMe_2Cl$ leads to the formation of the ion pairs of V(III) - direct precursors of the active species of polymerization [27-29]. Herewith, we summarize the results of these studies.

2. Experimental

All solvents used were dried over 3 Å and 4 Å molecular sieves, and were distilled in dry argon atmosphere. Vanadium(III) pre-catalysts **1** and **5** were synthesized via the reaction of the corresponding ligands with VCl_3 in THF media [17]. Organoaluminum co-catalysts ($AlMe_3$,

$AlMe_2Cl$, MAO) and $[Ph_3C][B(C_6F_5)_4]$ were purchased from Aldrich. $Al(CD_3)_3$ was synthesized by Dr. D. Babushkin according to the published procedure [30].

Ethylene polymerization was performed in a 0.3 L steel reactor. Solid pre-catalyst (~2 μmol) was introduced into the reactor in a sealed glass ampoule. The reactor was evacuated at 80 °C, cooled down to 20 °C and then charged with the freshly prepared solution of the co-catalyst in toluene or heptane. After setting up the desired temperature and ethylene pressure, the reaction was started by breaking the ampoule with the pre-catalyst. During the polymerization, ethylene pressure, temperature and stirring speed were maintained constant. The experimental unit was equipped with an automatic computer-controlled system for the ethylene feed, maintaining the required pressure, recording the ethylene consumption and providing the kinetic curve output both in the form of a table and as a graph. Weight-average (M_w) and number-average (M_n) molecular weights, and molecular weight distributions (M_w/M_n) were obtained by GPC measurements on a Waters-150 chromatograph at 150 °C, with trichlorobenzene as solvent. Viscosity (η) of the polymers was measured in decalin at 135 ºC on an Ubbelohde viscosimeter. The viscosity-average molecular weight M_v was calculated according to the Mark–Houwink equation: $M_v = (\eta/K)1/\alpha$, where the Mark–Hauwink coefficients $K = 67.7\times10^{-5}$; $\alpha = 0.67$.

The samples for NMR spectroscopy were prepared in the glovebox under an argon atmosphere. ^1H, ^2H, and ^{19}F NMR spectra were measured on a Bruker Avance 400 MHz NMR spectrometer at 400.130, 61.422, and 376.498 MHz, respectively, using 5 mm o.d. glass NMR tubes. ^1H chemical shifts were referenced to the residual peak of $CD_2HC_6D_5$ (δ 2.09); ^2H chemical shifts were referenced to the $CH_2DC_6H_5$ impurities (δ 2.1) in toluene; ^{19}F chemical shifts were referenced to the 1.2-difluorobenzene external standard (δ -139.0).

3. Results and discussion

Formation of the outer sphere and zwitter-ion like ion-pairs in the catalyst systems 1/$AlMe_3$/$[CPh_3]^+[B(C_6F_5)_4]^-$ and 1/MAO.

Bidentate *N*,*N*-donor *α*-diimine ligands were successfully used for the synthesis of the highly active nickel(II) and cobalt(II) complexes for ethylene oligomerization and polymerization [31, 32]. The ability of the V(III) complexes with *α*-diimine ligands to polymerize ethylene with moderate activity was previously demonstrated by Grassi et al. [17].

Complex **1** (L′VCl_3, where L′ = 1,4-bis-3,5-dimethylphenyl-2,3-dimethyl-1,4-diazabuta-1,3-diene) is a paramagnetic high-spin ($S = 1$) V(III) complex (Scheme 2). The ^{1}H NMR spectrum of **1** displays resonances of the *α*-diimine ligand (**A**, **B**, **C**, **E**, **A′**, **B′**, **C′**, **E′**), and those of one THF molecule, coordinated to the metal center (resonances **D** and **F**, Figure 1a and 1b). It is worth noting that **1** shows magnetic non-equivalence of the chemically equivalent ligand protons (**A-E**, **A'-E'**).

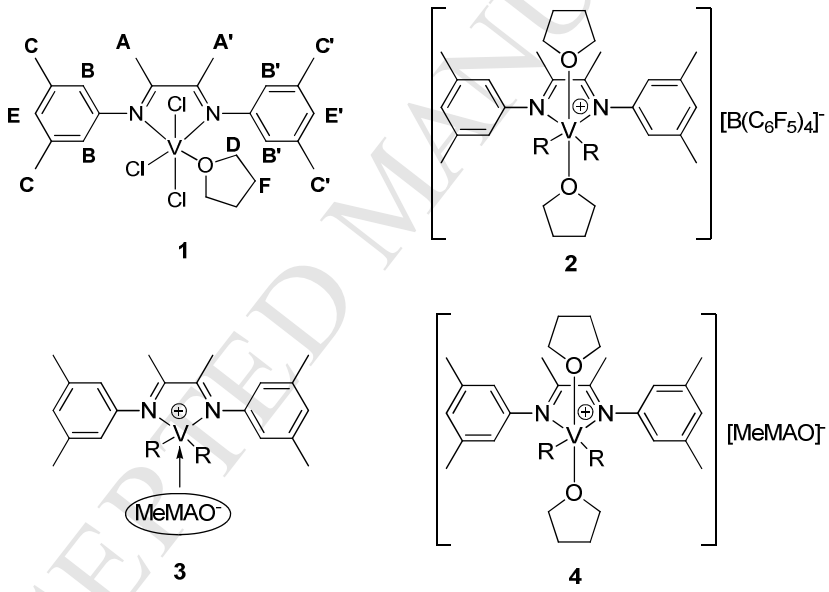

Scheme 2. Structure of pre-catalyst **1** considered in this work, and of complexes **2**-**4**.

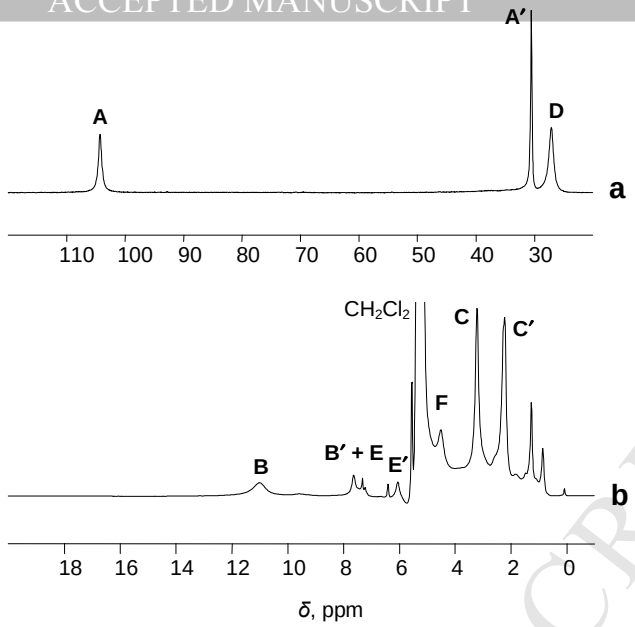

Figure 1. ^{1}H NMR spectrum of **1** (CH_2Cl_2, 25 °C, [V] = 0.01 M) in the 120 ppm to 20 ppm range (a), and in the 20 ppm to −1 ppm range (b). Peak assignment is given in Scheme 2.

Reaction of **1** with the $AlMe_3/[CPh_3]^+[B(C_6F_5)_4]^-$ co-catalyst ([V]:[Al]:[B] = 1:10:1.2) in 1,2-difluorobenzene/toluene-d_8 (1:3) media leads to a complete conversion of **1** to a new complex **2**, stable up to -20 °C. Using ^{1}H and ^{2}H NMR spectroscopy, it has been shown that **2** is an ion pair of the type $[L'V^{III}R_2(THF)_2]^+[B(C_6F_5)_4]^-$ (Scheme 2) where R = Me or Cl. The resonances of the ligand protons and two THF molecules have been detected and readily assigned (Figure 2).

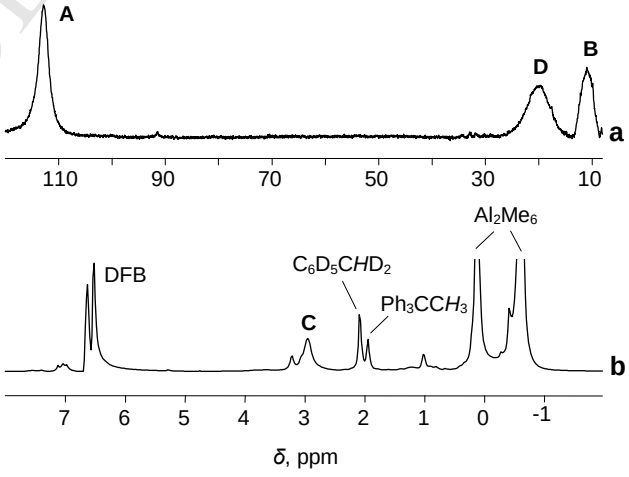

Figure 2. ^{1}H NMR spectrum (–40 °C, 1,2-difluorobenzene(DFB)/toluene-d_8 (1:3)) of the sample **1**/$AlMe_3$/$[Ph_3C][B(C_6F_5)_4]$ ([V]:[Al]:[B] = 1:10:1.2, [V] = 0.01 M, in the range 120 ppm to 8 ppm (a) and 8 ppm to –2 ppm (b). Peak assignment is given in Figure 2.

Unfortunately, the key resonance (resonances) of the Me group, directly bound to the vanadium center, was not detected even in the range of 1000 ppm to -1000 ppm. The absence of this signal in NMR does not rule out the presence of the V-Me moiety in the molecule of **2**: the dramatic line broadening can make this resonance unobservable by NMR. So, the exact nature of R remained unclear, however, rapid reduction of **2** even at -20 °C clearly indicated the presence at least one V-Me group. Unlike **1**, the molecule of **2** is more symmetric, demonstrating no magnetic non-equivalence of the ligand protons. Further $AlMe_3$ addition (up to 50 equiv.) to the sample **1**/$AlMe_3$/$[CPh_3]^+[B(C_6F_5)_4]^-$ does not lead to visible changes in the NMR spectrum.

Noteworthy, the system **1**/$AlMe_3$/$[CPh_3]^+[B(C_6F_5)_4]^-$ displays no ethylene polymerization activity. This is not surprising: strongly coordinated THF molecules occupy the coordination sites of the vanadium center, thus preventing ethylene coordination.

In contrast, the system **1**/MAO displays moderate activity toward ethylene polymerization (100 g PE /(mmol V·bar·min)), producing polyethylene with high molecular weight ($M_v \sim 6 \cdot 10^6$ g/mol). According to NMR data, the reaction of **1** with MAO leads to a new complex **3**. The NMR parameters of **2** and **3** noticeably differ: the resonance **A** of **3** ($\Delta\nu_{1/2} \sim 1600$ Hz) is much broader than that of **2** ($\Delta\nu_{1/2} \sim 590$ Hz). Only peaks of the bidentate ligand protons were detected; the resonances of the coordinated THF molecule or of V-Me moiety were not observed (Figure 3).

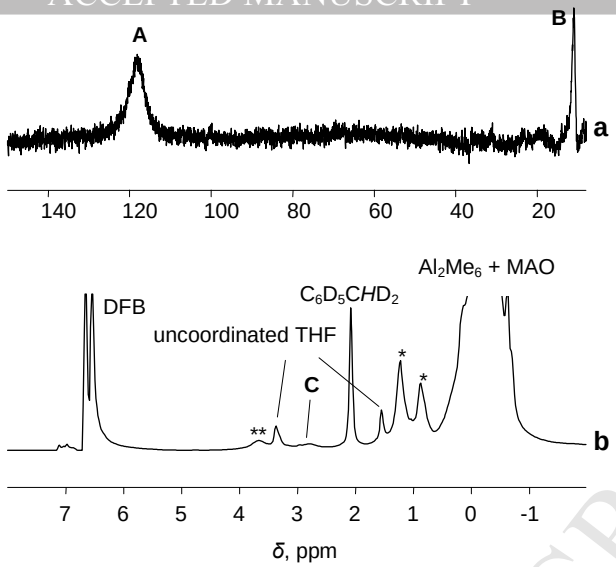

Figure 3. ^{1}H NMR spectrum of the sample **1**/MAO ([V]:[Al] = 1:40, [V] = 0.01 M, 1,2-difluorobenzene/toluene-d_8 (1:3), –40 °C) in the range 150 ppm to 8 ppm (a) and in the range 8 ppm to –2 ppm (b). Asterisks mark impurities of grease. Double asterisks mark impurities in MAO. Peak assignment is given in Scheme 2.

The addition of THF to the sample **1**/MAO leads to immediate disappearance of **3**, and buildup of resonances of a new complex **4**. Chemical shifts and line widths of the ^{1}H NMR resonances of **2** and **4** are almost identical, which suggests that **4** is most likely an ion pair of the type $[L'V^{III}R_2(THF)_2]^+[MeMAO]^-$, where R = Me or Cl (Scheme 2).

The dramatic broadening of the NMR resonances of **3** can be explained by tight $[MeMAO]^-$ coordination to the vanadium center, **3** being a zwitterion-like complex of the type $[L'V^{III}R_2^+\cdots MeMAO^-]$ (Scheme 2). The $[MeMAO]^-$ ligand in **3** is labile, thus allowing ethylene coordination to the vanadium center, followed by the V-R enchainment.

So, two sorts of ion pairs have been observed by ^{1}H NMR in the reaction of **1** with $AlMe_3/[CPh_3]^+[B(C_6F_5)_4]^-$ and MAO co-catalysts: the outer-sphere ion pairs of the type $[L'V^{III}R_2(THF)_2]^+[A]^-$ (**2** and **4**) and the zwitterion-like complex $[L'V^{III}R_2^+\cdots MeMAO^-]$ (**3**).

Formation of the ion pairs in the catalyst systems $5/AlMe_2Cl/[CPh_3]^+[B(C_6F_5)_4]^-$, $5/AlMe_2Cl$, $5/AlMe_3/[CPh_3]^+[B(C_6F_5)_4]^-$ and 5/MAO.

Previously, it was demonstrated that vanadium(III) complexes with bis(imino)pyridine ligands display much higher activity and stability in ethylene polymerization compared with *α*-diimine analogs 17, 33-35].

Like complex **1**, complex **5** ($LVCl_3$, where L = 2,6-bis[1-(2,6-dimethylphenylimino)ethyl]pyridine) is paramagnetic ($S = 1$), exhibiting broadened and paramagnetically shifted resonances in the ^1H NMR spectrum (Scheme 3, Figure 4). Unlike **1**, no magnetic non-equivalence of the chemically equivalent ligand protons of **5** was observed.

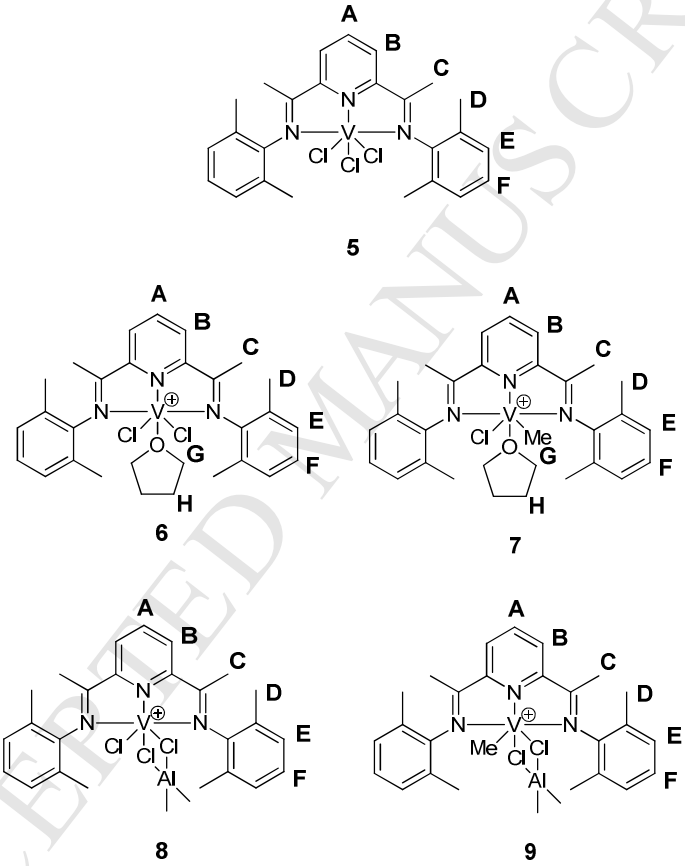

Scheme 3. Structure of pre-catalyst **5** considered in this work, and of cationic parts of species **6-9** (anionic parts are omitted for clarity).

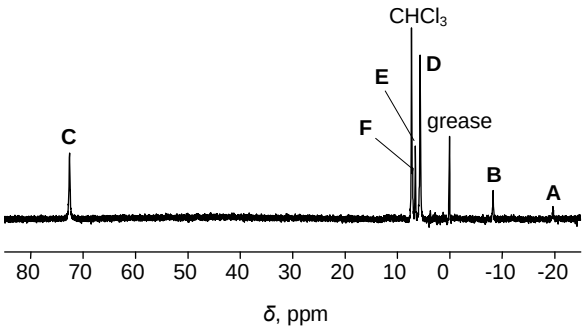

Figure 4. ^{1}H NMR spectrum of **5** ($CDCl_3$, 25 °C, [V] = 0.001 M). Peak assignment is given in Scheme 3.

Reaction of 5 with $AlMe_3/[CPh_3]^+[B(C_6F_5)_4]^-$ and $AlMe_2Cl/[CPh_3]^+[B(C_6F_5)_4]^-$ in the presence of THF

In attempt to stabilize the V(III) species formed upon the activation of **5** with $AlMe_3/[CPh_3]^+[B(C_6F_5)_4]^-$ and $AlMe_2Cl/[CPh_3]^+[B(C_6F_5)_4]^-$ systems, THF donor molecule was used. Specifically, the reaction of **5** with $AlMe_2Cl/[CPh_3]^+[B(C_6F_5)_4]^-$/THF led to complete conversion of **5** to a new highly stable complex **6**. According to ^{1}H, ^{2}H, and ^{19}F NMR data, **6** was assigned to the ion pair of the type $[LV^{III}Cl_2(THF)]^+[B(C_6F_5)_4]^-$, where L is the tridentate bis(imino)pyridine ligand (Figures 5 and 6, Scheme 3).

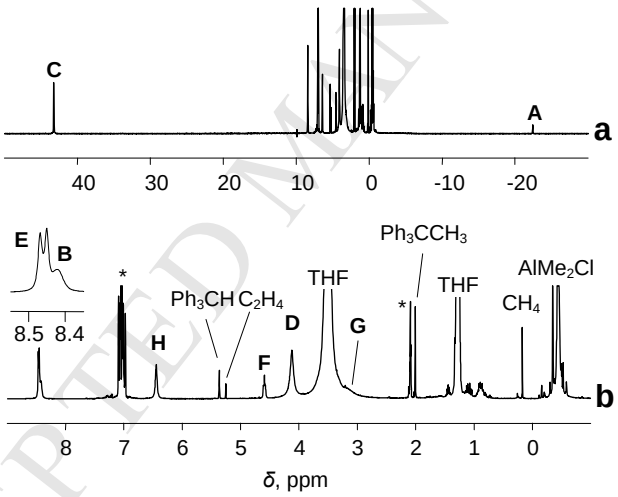

Figure 5. ^{1}H NMR spectrum (toluene-d_8, 25 °C) of the sample **5**/$AlMe_2Cl/[Ph_3C][B(C_6F_5)_4]$/THF ([V]:[Al]:[B]:[THF] = 1:15:1.2:35, [V] = 10^{-2} M) (a, b). Resonance assignment is given in Scheme 3.

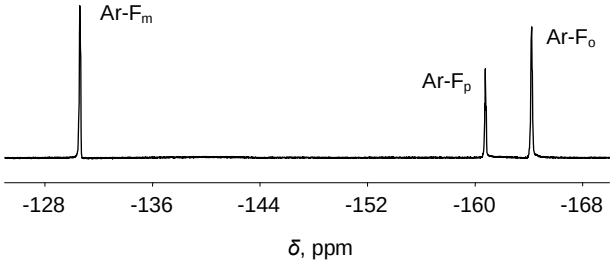

Figure 6. ^{19}F NMR spectrum (toluene-d_8, 25 °C) of the sample **5**/$AlMe_2Cl/[Ph_3C][B(C_6F_5)_4]$/THF ([V]:[Al]:[B]:[THF] = 1:15:1.2:35, [V] = 10^{-2} M).

The addition of $AlMe_3$ to the system **5**/$AlMe_2Cl$/$[CPh_3]^+[B(C_6F_5)_4]^-$/THF led to the formation of a new complex **7**, much less stable than **6**. Using ^1H and ^2H NMR spectroscopy, it was shown that **7** contains one V-Me group (Figure 7d). To the best of our knowledge, this is the first example of the ^1H and ^2H NMR spectroscopic detection of Me-group directly bound to V(III). So, **7** can be formulated as ion pair $[LV^{III}(Cl)Me(THF)]^+[B(C_6F_5)_4]^-$ (Schemes 3 and 4).

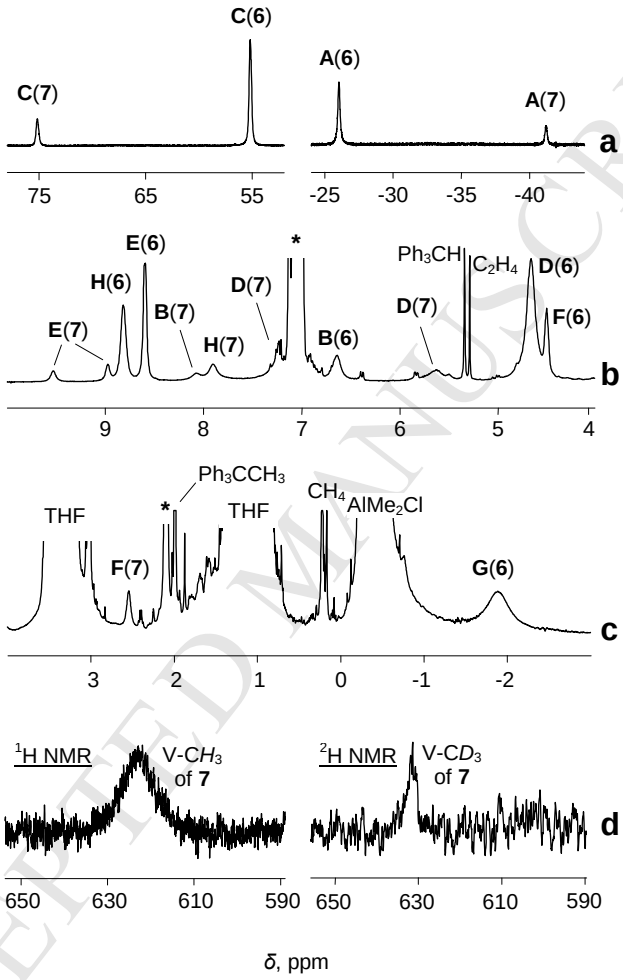

Figure 7. ^1H NMR spectrum (toluene-d_8, -20 °C) of the sample **5**/$AlMe_2Cl$/$[Ph_3C][B(C_6F_5)_4]$/THF/$AlMe_3$ ([V]:[$AlMe_2Cl$]:[B]:[THF]:[$AlMe_3$] = 1:15:1.2:35:15, [V] = 10^{-2} M) (a, b, c, d(left)). ^2H NMR spectrum (toluene, -20 °C) of the sample **5**/$AlMe_2Cl$/$[Ph_3C][B(C_6F_5)_4]$/THF/$Al(CD_3)_3$ ([V]:[$AlMe_2Cl$]:[B]:[THF]:[$Al(CD_3)_3$]= 1:15:1.2:35:15) (d(right)). Asterisks mark peaks of residual protons in toluene-d_8. Peak assignment is given in Scheme 3.

The reaction of **5** with $AlMe_3/[CPh_3]^+[B(C_6F_5)_4]^-$ in the presence of THF also led to the appearance of complexes **6** and **7**; fully methylated $[LV^{III}Me_2(THF)]^+[B(C_6F_5)_4]^-$ was not observed, probably due to its insufficient stability even at low temperatures.

The systems **5**/$AlMe_3/[CPh_3]^+[B(C_6F_5)_4]^-$/THF and **5**/$AlMe_2Cl/[CPh_3]^+[B(C_6F_5)_4]^-$/THF are inactive toward ethylene. Like in the case of the **1**/$AlMe_3/[CPh_3]^+[B(C_6F_5)_4]^-$ system, strongly coordinating THF blocks the access of ethylene to the vanadium center.

Reaction of 5 with $AlMe_3/[CPh_3]^+[B(C_6F_5)_4]^-$ and $AlMe_2Cl/[CPh_3]^+[B(C_6F_5)_4]^-$ in the absence of THF

Practical catalyst systems of ethylene polymerization contain no THF. So, the reactions between **5** and $AlMe_3/[CPh_3]^+[B(C_6F_5)_4]^-$ and $AlMe_2Cl/[CPh_3]^+[B(C_6F_5)_4]^-$ co-catalysts were studied in the absence of THF. The reaction of **5** with $AlMe_2Cl/[CPh_3]^+[B(C_6F_5)_4]^-$ leads to the paramagnetic complex **8**, stable at room temperature. When THF was added to **8**, the latter immediately converted to species **6**. On the other hand, when an excess (15 equiv.) of $AlMe_2Cl$ was added to the resulting sample, **6** converted back to **8**.

According to the NMR data (Figure 8), **8** contains the bis(imino)pyridine ligand and one $AlMe_2Cl$ molecule. One can conclude that **8** and **6** differ in the nature of the additional coordinated molecules: THF in the case of **6** and $AlMe_2Cl$ in the case of **8**. So, **8** can be assigned to a heterobinuclear ion pair of the type $[LV^{III}(Cl)(\mu\text{-}Cl)_2AlMe_2]^+[B(C_6F_5)_4]^-$ where L is the tridentate bis(imino)pyridine ligand (Schemes 3 and 4).

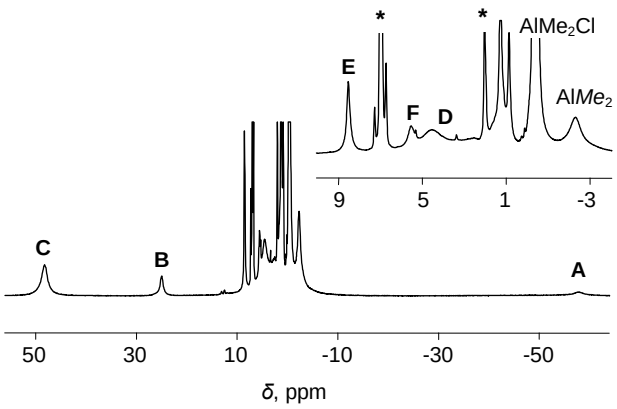

Figure 8. ^{1}H NMR spectrum (toluene-d_8, 25 °C) of the sample **5**/$AlMe_2Cl$/$[Ph_3C][B(C_6F_5)_4]$ ([V]:[$AlMe_2Cl$]:[B] = 1:15:1.2, [V] = 10^{-2} M). Asterisks mark peaks of residual protons in toluene-d_8. Peak assignment is given in Scheme 3.

^{1}H NMR spectra of the sample **5**/$AlMe_3$/$[CPh_3]^+[B(C_6F_5)_4]^-$ display resonances of a new complex **9** (Figure 9a). Unlike **8,** this complex displays low stability and can be observed in the reaction mixture only at low temperatures (below -20 °C). The addition of $AlMe_2Cl$ to the sample containing **9** converts the latter into **8**. On the contrary, the addition of excess of $AlMe_3$ converts **8** back into **9**. When THF was added to the solution containing **9**, formation of a mixture of **6** and **7** was observed. The ^{1}H NMR spectrum of **9** displays resonances of the bis(imino)pyridine ligand and the $AlMe_2$ moiety. To justify the assignment of the resonance at δ -2.9 to the $AlMe_2$ group, the sample **5**/$Al(CD_3)_3$/$[CPh_3]^+[B(C_6F_5)_4]^-$ was studied by ^{2}H NMR spectroscopy. As it was expected, ^{2}H NMR spectrum of the sample **5**/$Al(CD_3)_3$/$[CPh_3]^+[B(C_6F_5)_4]^-$ ([V]:[Al]:[B] = 1:15:1.2), recorded at -20 °C, displayed the resonance at δ -2.9, corresponding to the $AlMe_2$ moiety (Figure 9b). This experiment indicates that the resonance at δ -2.9 belongs to the $AlMe_2$ group, and supports the assignment of **9** to the heterobinuclear ion pair $[LV^{III}(Me)(\mu\text{-}Cl)_2AlMe_2]^+[B(C_6F_5)_4]^-$ where L is the bis(imino)pyridine ligand (Schemes 3 and 4). The low stability of **9** is caused by the presence of the V-Me group.

Possible transformations of **5** upon reaction with $AlMe_2Cl$/$[Ph_3C][B(C_6F_5)_4]$ and $AlMe_3$/$[Ph_3C][B(C_6F_5)_4]$ in presence and absence of THF are summarized in Scheme 4.

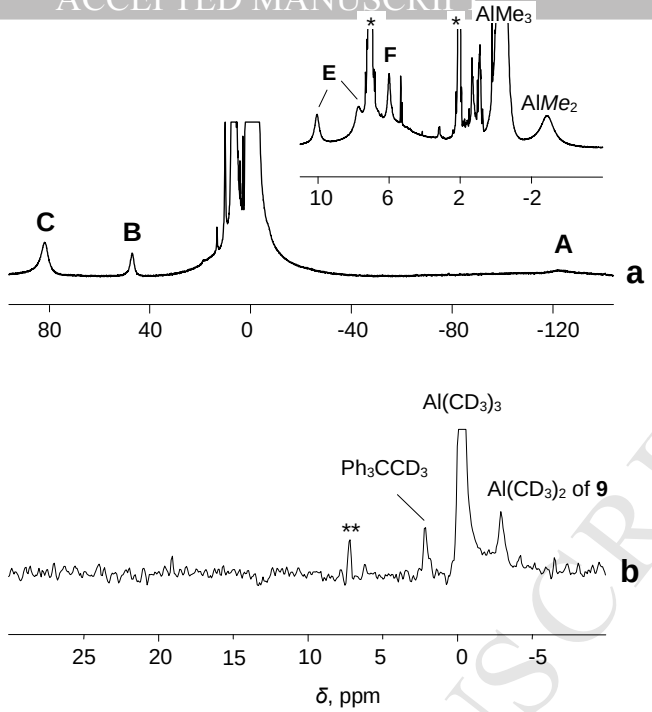

Figure 9. ^{1}H NMR spectrum (toluene-d_8, -20 °C) of the sample **5**/$AlMe_3$/$[Ph_3C][B(C_6F_5)_4]$ ([V]:[Al]:[B] = 1:15:1.2, [V] = 10^{-2} M) (a). ^{2}H NMR spectrum (toluene, -20 °C) of the sample **5**/$Al(CD_3)_3$/$[CPh_3]^+[B(C_6F_5)_4]^-$ ([V]:[Al]:[B] = 1:10:1.2, [V] = 10^{-2} M). Asterisks mark peaks of residual protons in toluene-d_8. Double asterisks mark peak of $CH_3C_6H_4D$.

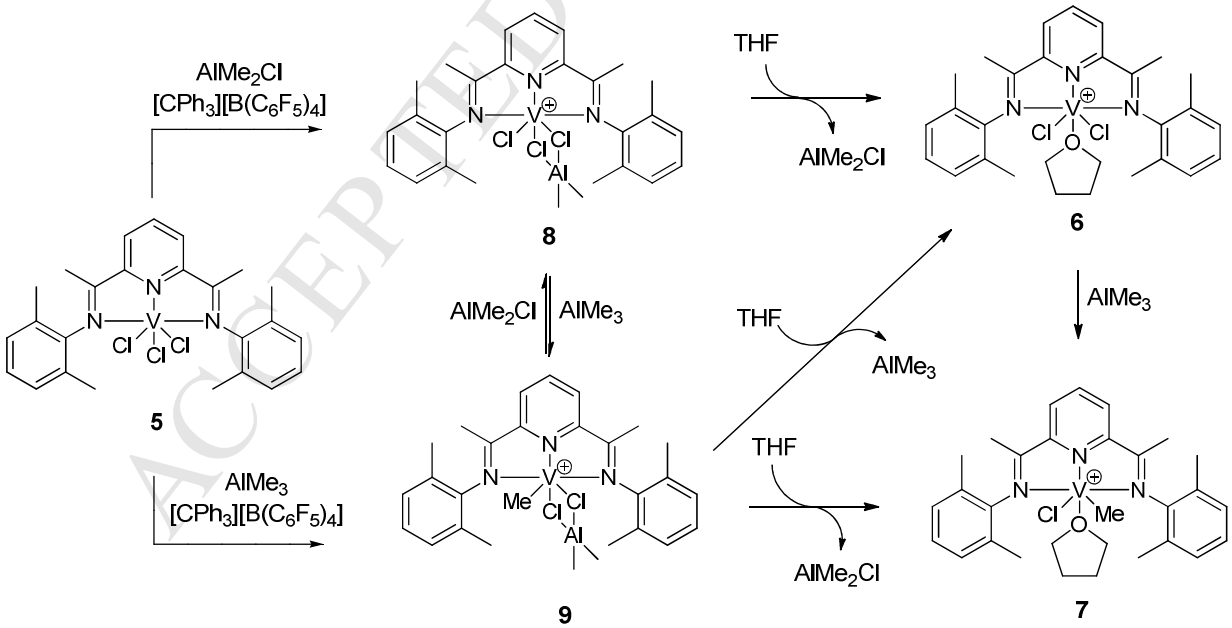

Scheme 4. Transformations of complex **5** during reactions with $AlMe_2Cl$/$[Ph_3C][B(C_6F_5)_4]$ and $AlMe_3$/$[Ph_3C][B(C_6F_5)_4]$ in the presence and absence of THF. Only cationic parts are shown, anionic parts are omitted for clarity.

Reaction of 5 with $AlMe_2Cl$

^{1}H NMR spectrum of the system **5**/$AlMe_2Cl$ (Figure 10) displays resonances of two paramagnetic complexes **8′** (major product) and **9′** (minor product). The NMR spectra of **8** and **8′** are almost identical, which clearly reflects the similarity of their structures. The same is true for complexes **9** and **9′**. Plausibly, **8′** and **9′** are heterobinuclear ion pairs of the types $[LV^{III}(Cl)(\mu\text{-}Cl)_2AlMe_2]^+[AlMe_3Cl]^-$ and $[LV^{III}(Me)(\mu\text{-}Cl)_2AlMe_2]^+[AlMe_3Cl]^-$, respectively (Scheme 5). The ratio between **8′** and **9′** can be manipulated by the addition of $AlMe_3$ to the reaction mixture.

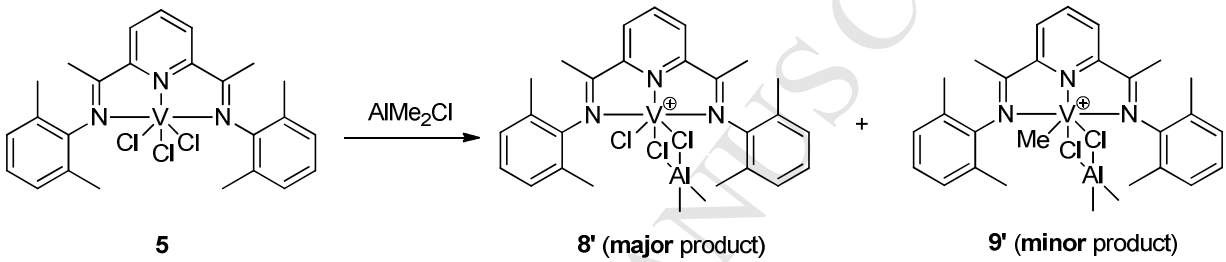

Scheme 5. Transformations of complex **5** into **8′** and **9′** upon reaction with $AlMe_2Cl$. Cationic part are shown, anionic part is omitted for clarity.

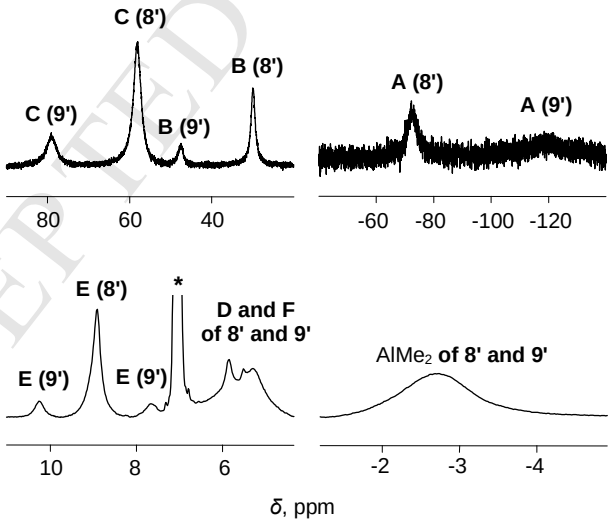

Figure 10. ^{1}H NMR spectrum (toluene-d_8, –20 °C, expanded regions) of the sample **5**/$AlMe_2Cl$ ([V]:[Al] = 1:15, [V] = 10^{-2} M). Asterisk marks peak of the residual protons in toluene-d_8.

Reaction of 5 with MAO

The highest activity of **5** in ethylene polymerization was achieved using MAO as a co-catalyst (Table 1). Therefore, it is important to obtain data on the structure of vanadium species formed in the system **5**/MAO.

Table 1.

Ethylene polymerization over complex **1** with different co-catalysts. [a]

Entry	Co-catalyst	[Al]/[V]	$P(C_2H_4)$, bar	Activity, $g_{PE}/(mmol_V \cdot h)$	M_n, g/mol	M_W, g/mol	M_w/M_n
1	MAO	500	1	15 600	1 600	4 300	2.7
2	$AlMe_3$/ $[Ph_3C][B(C_6F_5)_4]$	100[b]	2	3 300	1 800	3 700	2.1
3	$AlMe_2Cl$/ $[Ph_3C][B(C_6F_5)_4]$	200[b]	2	-	-	-	-
4	$AlMe_2Cl$	200	2	-	-	-	-

[a] Conditions: toluene (entries 1, 2, 3, 50 mL) or heptane (entry 4, 100 ml); polymerization temperature 60 °C; 2 μmol of V; polymerization time 60 min (30 min for entry 1)

[b] The molar ratio $[V]/[Ph_3C][B(C_6F_5)_4]$ is 1:1.2.

The ^{1}H NMR spectrum of the sample **5**/MAO ([V]:[Al] = 1:20), recorded at -20 °C, is presented in Figure 11. Some of the ^{1}H resonances of a new vanadium complex **10** formed in this sample are obscured by the intense peaks of MAO and toluene (solvent of commercial MAO). Nevertheless, the key resonances of **10** can be detected. These resonances coincide with the corresponding resonances of **9** and **9′** (Table 2). So, complex **10** can be reasonably assigned to the ion pair $[L(Me)V^{III}(\mu\text{-}Cl)_2AlMe_2]^+[MeMAO]^-$ (Scheme 6). This is the first reported example of characterization of such species in catalyst systems of the type $LV^{III}Cl_3$/MAO (L = bis(imino)pyridine ligand).

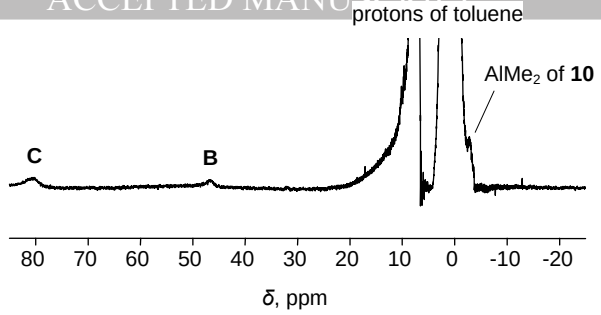

Figure 11. ^{1}H NMR spectrum (toluene-d_8, −20 °C) of the sample **5**/MAO ([V]:[Al] = 1:20, [V] = 10^{-2} M).

Table 2

Selected ^{1}H NMR parameters (δ, ppm and $\Delta\nu_{1/2}$, Hz) of complexes 9, 9′, and 10 at -20 °C.

complex		C	B	$AlMe_2$
9	δ	80.9	46.9	–2.9
	$\Delta\nu_{1/2}$	1270	670	350
9'	δ	79.0	47.6	–2.7
	$\Delta\nu_{1/2}$	1060	550	~360
10	δ	~81	~47	~ –2.9
	$\Delta\nu_{1/2}$	~100	~600	not measured

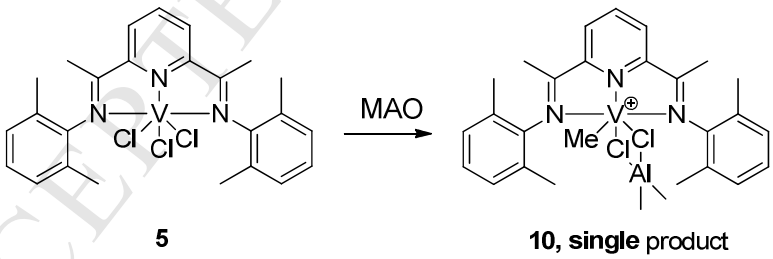

Scheme 6. Formation of complex **10** in the system **5**/MAO. In **10**, anionic part is omitted for clarity.

Ethylene polymerization over catalyst 5 and possible nature of the active species

As it was mentioned above, **5** displays high ethylene polymerization activity (15 600 *g* PE/(mmol V·bar·h)) upon the activation with MAO (Table 1). The resulting polyethylene has low molecular weight (M_w = 4 300 g/mol) and narrow molecular-weight distribution (M_w/M_n = 2.7), characteristic of nearly single-site catalysts. The model catalysts system

5/$AlMe_3$/[CPh_3][$B(C_6F_5)_4$] displays much lower activity (3 300 *g* PE/(mmol V· h)) but produces PE with similar molecular weight (M_w = 3 700 g/mol) and MWD (M_w/M_n = 2.1). The catalyst systems based on complex **5** displays much higher stability, than those based on complex **1**.

Only traces of polymeric product were obtained using the catalyst systems **5**/$AlMe_2Cl$ and **5**/$AlMe_2Cl$/[CPh_3][$B(C_6F_5)_4$]. The systems **5**/$AlMe_3$/[CPh_3][$B(C_6F_5)_4$]/THF and **5**/$AlMe_2Cl$/[CPh_3][$B(C_6F_5)_4$]/THF did not display ethylene polymerization activity.

These results agree with the NMR data. In the case of the systems **5**/MAO and **5**/$AlMe_3$/[Ph_3C][$B(C_6F_5)_4$], the major part of vanadium exists in the reaction solution in the form of the heterobinuclear ion pairs of the types **9** and **10**, $[L(Me)V^{III}(\mu\text{-}Cl)_2AlMe_2]^+[A]^-$ (**9**: $[A]^-$ = $[B(C_6F_5)_4]^-$, **10**: $[A]^-$ = $[MeMAO]^-$). These complexes contain V^{III}-CH_3 moiety and can be the closest precursors of the active species of polymerization.

On the contrary, in the systems **5**/$AlMe_2Cl$/[Ph_3C][$B(C_6F_5)_4$] and **5**/$AlMe_2Cl$, the major part of vanadium exists in the form of the heterobinuclear ion pairs of the types **8** and **8′**, $[L(Cl)V^{III}(\mu\text{-}Cl)_2AlMe_2]^+[A]^-$ (**8**: $[A]^-$ = $[B(C_6F_5)_4]^-$, **8′**: $[A]^-$ = $[AlMe_3Cl]^-$). Species **8** and **8′** contain no vanadium-alkyl bond and thus are unable to promote ethylene enchainment; in effect, the corresponding catalyst systems display very low catalyst activity.

Discussion of deactivation pathways of the catalyst systems studied

There are several deactivation pathways of the vanadium based catalyst systems postulated in the literature. The major ones are the following: (a) reduction of the vanadium(III) center to polymerization-inactive low-valent state (II, I, 0) and (b) ligand transfer from V to Al [2, 4, 5, 17]. The *in situ* ^1H NMR investigation of the catalyst system **5**/$AlMe_3$/[Ph_3C][$B(C_6F_5)_4$] in the presence of ethylene has shown that PE formation is accompanied by the emergence of a new diamagnetic complex $[LAlMe_2]^+[B(C_6F_5)_4]^-$ - the product of the bis(imino)pyridine ligand transfer to aluminum (Figure 12, Scheme 7). This ligand transfer from V to Al is apparently the predominant deactivation pathway for complex **5**.

On the other hand, warming the catalyst system **5**/$AlMe_3$/$[Ph_3C][B(C_6F_5)_4]$ up to room temperature in the absence of ethylene leads to the disappearance of complex **9**. At the same time, ^1H NMR spectra show the emergence of the ethane (δ 0.86) and methane (δ 0.17) resonances, which indicates the homolytic splitting of V^{III}-CH_3, resulting in the formation of catalytically inactive V^{II} species [2]. The structure of the low-valent vanadium species present in the reaction remains unclear.

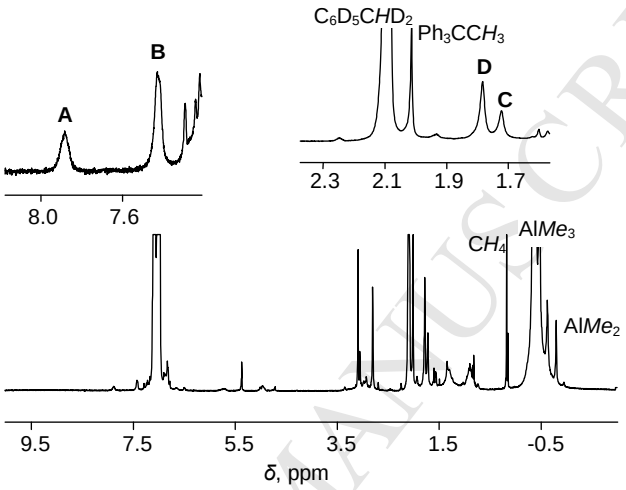

Figure 12. ^1H NMR spectrum (toluene-d_8, 25 °C) of the complex $[LAlMe_2]^+[B(C_6F_5)_4]^-$ observed in the catalyst system **5**/$AlMe_3$/$[Ph_3C][B(C_6F_5)_4]$/C_2H_4 ([V]:[Al]:[B] = 1:15:1.2; N(V):N(C_2H_4) = 1:50).

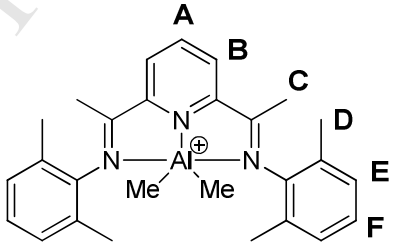

Scheme 7. The structure of complex $[LAlMe_2]^+[B(C_6F_5)_4]^-$ (cationic part, anionic part is omitted for clarity).

4. Conclusions

The ion pairs formed upon the reactions of α-diimine (**1**) and bis(imino)pyridine (**5**) vanadium(III) pre-catalysts with MAO, $AlMe_2Cl$, $AlMe_2Cl$/$[Ph_3C][B(C_6F_5)_4]$, and $AlMe_3$/$[Ph_3C][B(C_6F_5)_4]$, were characterized in detail by ^1H, ^2H, and ^{19}F NMR spectroscopy,

including the ^{1}H and ^{2}H NMR observation of the V^{III}-CH_3 moiety. For complex **1**, zwitterion-like complexes $[L'V^{III}R_2^{+}\cdots MeMAO^{-}]$ and ion pairs $[L'V^{III}R_2(THF)_2]^{+}[A]^{-}$ (L′ = 1,4-bis-3,5-dimethylphenyl-2,3-dimethyl-1,4-diazabuta-1,3-diene; $[A]^{-}$ = $[MeMAO]^{-}$ or $[B(C_6F_5)_4]^{-}$) have been identified. In the systems based on the complex **5**, ion pairs of the type $[L(Cl)V^{III}(\mu\text{-}Cl)_2AlMe_2]^{+}[A]^{-}$, $[L(Me)V^{III}(\mu\text{-}Cl)_2AlMe_2]^{+}[A]^{-}$, $[LV^{III}Cl_2(THF)]^{+}[A]^{-}$ and $[LV^{III}(Cl)Me(THF)]^{+}[A]^{-}$ (L = 2,6-bis[1-(2,6-dimethylphenylimino)ethyl]pyridine; $[A]^{-}$ = $[AlMe_3Cl]^{-}$ or $[B(C_6F_5)_4]^{-}$) were detected.

The proposed structure of the ion-pairs formed in the catalyst systems studied readily explain their catalytic properties. Indeed, catalyst systems exhibiting ion pairs incorporating V^{III}-Me moieties display high ethylene polymerization activity, whereas catalyst systems displaying predominantly intermediates containing no V^{III}-Me moieties are virtually inactive toward ethylene.

Formation of the aluminum complex of the type $[LAlMe_2]^{+}[B(C_6F_5)_4]^{-}$ (L = bis(imino)pyridine ligand) in the **5**/$AlMe_3$/$[Ph_3C][B(C_6F_5)_4]$/C_2H_4 in the course of ethylene polymerization, formed upon ligand transfer from V to Al, reflects the importance of this catalyst deactivation pathway.

Conflict of interest

The authors declare no competing financial interest.

Acknowledgements

This work was supported by the Russian Foundation for Basic Research (grant 16-03-00236). The NMR measurements and polymerization experiments were performed using the equipment of the Russian Academy of Sciences and the Federal Agency for Scientific Organizations (project 0303-2016-0009). The authors thank Dr. M.A. Matsko for the polymer MWD analysis, and Dr. D.E. Babushkin for fruitful discussions and for the $Al(CD_3)_3$ synthesis. Technical assistance from Mrs. T.G. Ryzhkova is gratefully acknowledged.

References

[1] S.C. Davis, W. von Hallens, H. Zahalka, Polymer material encyclopedia, Vol. 3 (Ed.: J. Salamone), CRS Press, Boca Raton, 1996.

[2] S. Gambarotta, Coord. Chem. Rev. 237 (2003) 229-243.

[3] J.W.M. Noordermeer in Kirk-Othmer Encyclopedia of Chemical Technology, Vol. 10, 5th Edition (Ed.: Kirk-Othmer) J. Wiley & Sons, New York, 2005, p. 704-719.

[4] C. Redshaw, Dalton Trans. 39 (2010) 5595-5604.

[5] K. Nomura, S. Zhang, Chem. Rev. 111 (2011) 2342-2362.

[6] L. Clowes, M. Walton, C. Redshaw, Y.M. Chao, A. Walton, P. Elo, V. Sumerin, D.L. Hughes, Cat. Sci. Tech. 3 (2013) 152-160.

[7] J. Ma, K.Q. Zhao, M. Walton, J.A. Wright, D.L. Hughes, M.R.J. Elsegood, K. Hughes, X.S. Sun, C. Redshaw, Dalton Trans., 43 (2014) 16698-16706.

[8] J. Ma, K.Q. Zhao, M.J. Walton, J.A. Wright, J.W.A. Frese, M.R.J. Elsegood, Q.F. Xing, W.H. Sun, C. Redshaw, Dalton Trans. 43 (2014) 8300-8310.

[9] C. Redshaw, M.J. Walton, M.R.G. Elsegood, T.J. Prior, K. Michiue, RSC Adv. 5 (2015) 89783-89796.

[10] C. Redshaw, M. Walton, K. Michiue, Y.M. Chao, A. Walton, P. Elo, V. Sumerin, C.Y. Jiang, M.R.G. Elsegood, Dalton Trans. 44 (2015) 12292-12303.

[11] C. Redshaw, M.J. Walton, D.S. Lee, C.Y. Jiang, M.R.J. Elsegood, K. Michiue, Chem. Eur. J. 21 (2015) 5199-5210.

[12] M.D. Leatherman, S.A. Svejda, L.K. Johnson, M.J. Brookhart, Am. Chem. Soc. 125 (2003) 3068-3081.

[13] M. Bochmann, Organometallics 29 (2010) 4711-4740.

[14] K.P. Bryliakov, E.P. Talsi, Coord. Chem. Rev.256 (2012) 2994-3007.

[15] A.A. Antonov, D.G. Samsonenko, E.P. Talsi, K.P. Bryliakov, Organometallics 32 (2013) 2187-2191.

[16] I.E. Soshnikov, N.V. Semikolenova,V.A. Zakharov, H.M. Moller, F. Olscher, A. Osichow, I. Gottker-Schnettmann, S. Mecking, E.P. Talsi, K.P. Bryliakov, Chem. Eur. J. 19 (213) 11409-11417.

[17] S. Milone, G. Cavallo, C. Tedesco, A. Grassi, J. Chem. Soc. Dalton Trans. (2002) 1839-1846.

[18] I.E. Soshnikov, N.V. Semikolenova, K.P. Bryliakov, A.A. Shubin, V.A. Zakharov, C. Redshaw, E.P. Talsi, Macromol. Chem. Phys. 210 (2009) 542-548.

[19] I.E. Soshnikov, N.V. Semikolenova, K.P. Bryliakov, V.A. Zakharov, C. Redshaw, E.P. Talsi, J. Mol. Cat. A, Chem. 303 (2009) 23-29.

[20] I.E. Soshnikov, N.V. Semikolenova, A.A. Shubin, K.P. Bryliakov, V.A. Zakharov, C. Redshaw, E.P. Talsi, Organometallics 28 (2009) 6714-6720.

[21] A. Igarashi, S. Zhang, K. Nomura, Organometallics 31 (2012) 3575-3581.

[22] E.A.C. Brussee, A. Meetsma, B. Hessen, J.H. Teuben, Organometallics 17 (1998) 4090-4095.

[23] G.K.B. Clentsmith, V.M.E. Bates, P.B. Hitchcock, F.G.N. Cloke, J. Am. Chem. Soc. 121 (1999) 10444-10445.

[24] R. Choukroun, C. Lorber, B. Donnadieu, Organometallics 21 (2002) 1124-1126.

[25] W-K. Kim, M.J. Fevola, L.M. Liable-Sands, A.L. Rheingold, K.H. Theopold, Organometallics, 17 (1998) 4541-4543.

[26] (a) K. Nomura,T. Mitsudome, A. Igarashi,G. Nagai, K. Tsutsumi, T. Ina, T. Omiya, H. Takaya, S. Yamazoe, Organometallics 36 (2017) 530-542.
(b) J. Campos, J. Lopes-Serrano, R. Peloso, E. Carmona, Chem. Eur. J. 22 (2016) 6432-6457.

[27] I.E. Soshnikov, N.V. Semikolenova, A.A. Antonov, K.P. Bryliakov, V.A. Zakharov, E.P. Talsi, Organometallics 33 (2014) 2583-2587.

[28] I.E. Soshnikov, N.V. Semikolenova, K.P. Bryliakov, V.A. Zakharov, E.P. Talsi, J. Mol. Catal. A: Chem. 423 (2016) 333-338.

[29] I.E. Soshnikov, N.V. Semikolenova, K.P. Bryliakov, V.A. Zakharov, E.P. Talsi, ChemCatChem, 9 (2017) 1253-1260.

[30] E.P. Talsi, D.E. Babushkin, N.V. Semikolenova, V.N. Zudin, V.A. Zakharov, Kinet. Catal. 42 (2001) 147-153.

[31] S.D. Ittel, L.K. Johnson, M. Brookhart, Chem. Rev. 100 (2000) 1169-1204(and ref. therein)

[32] V. Rosa, S.A. Carabineiro, T. Aviles, P.T. Gomes, R. Welter, J.M. Campos, M.R.Ribeiro, J. Organomet. Chem. 693 (2008) 769-775.

[33] D. Reardon, F. Conan, S. Gambarotta, G. Yap, Q. Wang, J. Am. Chem. Soc. 121 (1999) 9318-9325.

[34] R. Schmidt, M.B. Welch, R.D. Knudsen, S. Gottfried, H.G. Alt, J. Mol. Catal. A 222 (2004) 17-25.

[35] J.R.V. Lang, C.E. Denner, H. G. Alt, J. Mol. Catal. A. 322 (2010) 45-49.

Highlights

- The species formed upon activation of vanadium(III) pre-catalysts were detected by NMR
- The structures of these species were proposed
- The nature of the active sites and deactivation pathways are discussed